Attosecond Control of Restoration of Electronic Structure Symmetry

ChunMei Liu,[1] Jörn Manz,[1,2,3,*] Kenji Ohmori,[4,5,†] Christian Sommer,[4,5,6]
Nobuyuki Takei,[4,5] Jean Christophe Tremblay,[1] and Yichi Zhang[2,3,4]
[1]*Freie Universität Berlin, Institut für Chemie und Biochemie, 14195 Berlin, Germany*
[2]*State Key Laboratory of Quantum Optics and Quantum Optics Devices, Institute of Laser Spectroscopy, Shanxi University, Taiyuan 030006, China*
[3]*Collaborative Innovation Center of Extreme Optics, Shanxi University, Taiyuan 030006, China*
[4]*Institute for Molecular Science, National Institutes of Natural Sciences, Myodaiji, Okazaki 444-8585, Japan*
[5]*SOKENDAI (The Graduate University of Advanced Studies), Myodaiji, Okazaki 444-8585, Japan*
[6]*Max-Planck-Institut für die Physik des Lichts, 91058 Erlangen, Germany*

(Received 23 March 2018; published 25 October 2018)

Laser pulses can break the electronic structure symmetry of atoms and molecules by preparing a superposition of states with different irreducible representations. Here, we discover the reverse process, symmetry restoration, by means of two circularly polarized laser pulses. The laser pulse for symmetry restoration is designed as a copy of the pulse for symmetry breaking. Symmetry restoration is achieved if the time delay is chosen such that the superposed states have the same phases at the temporal center. This condition must be satisfied with a precision of a few attoseconds. Numerical simulations are presented for the C_6H_6 molecule and ^{87}Rb atom. The experimental feasibility of symmetry restoration is demonstrated by means of high-contrast time-dependent Ramsey interferometry of the ^{87}Rb atom.

DOI: 10.1103/PhysRevLett.121.173201

The purpose of this Letter is to show that well-designed laser pulses can not only break (see, e.g., Refs. [1–7]) but also restore the electronic symmetry of atoms and molecules. This presents a new challenge in coherent control [8–10]. Controlling the electronic symmetry may be used in chemical reaction [11–14] and charge migration [15,16]. In retrospect, there are already implicit solutions, e.g., in early work on Ramsey fringes [17,18], or high harmonic generation [19–23], but the authors did not note the phenomenon. We shall first derive the theory for two laser pulses that break and restore symmetry, with applications to two model systems that have highly symmetric ground states: the benzene molecule and the ^{87}Rb atom. Subsequently, we shall demonstrate its feasibility by a high-contrast Ramsey interferometry experiment applied to ^{87}Rb. As by-product, the results will add a fascinating effect to attosecond (as) science [6,7,21–23].

As a proof of principle, we consider the scenario where symmetry is broken (b) and restored (r) by two right circularly polarized laser pulses that are well separated from each other, with maximum intensities at $t_b < 0$ and at $t_r = -t_b$. The time delay is $t_d = t_r - t_b$. The electric field for symmetry restoration ϵ_r is designed as a copy of the field ϵ_b for symmetry breaking,

$$\epsilon_r(t + t_r) = \epsilon_b(t + t_b). \tag{1}$$

The total electric field is $\epsilon(t) = \epsilon_b(t) + \epsilon_r(t)$, with intensity $I(t) = (1/2)c\varepsilon_0|\epsilon(t)|^2$. It is negligible—that means the system is in a quasi-field-free environment—at initial ($t_i < t_b$), "central" [$t_c = 0.5\,(t_b + t_r) = 0$], and final times ($t_f = -t_i$). For convenience, all pulses have Gaussian envelopes, or they are constructed as superposition of two Gaussian subpulses labeled $j = 1, 2$, with the same amplitudes $\epsilon^{(j)} = \epsilon_b^{(j)} = \epsilon_r^{(j)}$, carrier frequencies $\omega_c^{(j)} = \omega_{cb}^{(j)} = \omega_{cr}^{(j)}$, and durations $\tau^{(j)} = \tau_b^{(j)} = \tau_r^{(j)} \ll t_d$. The carrier envelope phases are set equal to zero, $\eta_{bx}^{(j)} = \eta_{by}^{(j)} = \eta_{rx}^{(j)} = \eta_{ry}^{(j)} = 0$. For example,

$$\vec{\epsilon}_b(t) = \epsilon e^{-(t-t_b)^2/2\tau^2}\{\cos[\omega_c(t-t_b)]\vec{e}_x + \sin[\omega_c(t-t_b)]\vec{e}_y\}. \tag{2}$$

As a consequence, the matrix representation of the Hamiltonian of the system (s) with semiclassical dipole coupling to the laser field, $H(t) = H_s - \vec{d}\cdot\vec{\epsilon}(t)$ is adjunct upon time reversal (see the Supplemental Material [24])

$$\mathbf{H}(t) = \mathbf{H}^*(-t). \tag{3}$$

Our scenario focuses on the laser driven electron dynamics for fixed nuclei. It starts with the system in its ground (g) state, with wave function $\Psi(t_i) = \Psi_g$, energy $E_g(= 0)$, and irreducible representation IRREP$_g$. The first laser pulse breaks symmetry by exciting the system to a superposition $\Psi(t) = c_g(t)\Psi_g + c_e(t)\Psi_e$ of Ψ_g and an excited state Ψ_e with energy E_e, and with populations

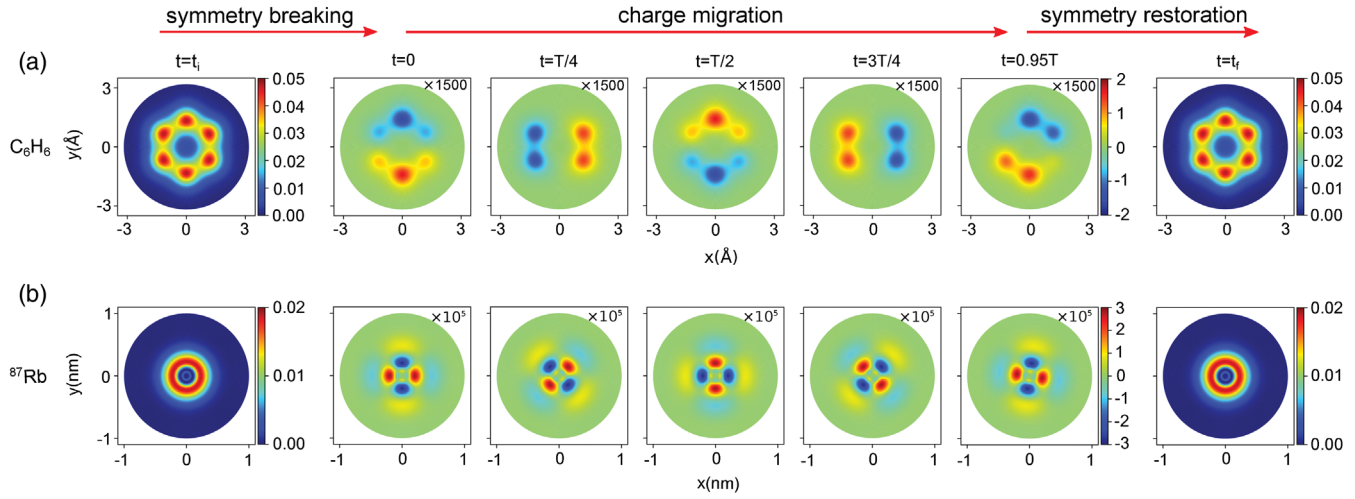

FIG. 1. Evolution of the electronic density upon laser-induced symmetry breaking, charge migration, and symmetry restoration. The central panels show snapshots of the time-dependent part of the electronic density in the superposition state $C_g e^{i\eta_g} e^{-iE_g t/\hbar}\psi_g + C_e e^{i\eta_e} e^{-iE_e t/\hbar}\psi_e$, $|C_e|^2 = 0.0037$. Time $t_c = 0$ is chosen to satisfy condition (5). (a) Application to C_6H_6: $D_{6h} \rightarrow C_s \rightarrow D_{6h}$. (b) Application to ^{87}Rb: isotropic → anisotropic → isotropic. The laser parameters are in Figs. 2 and 3, legends.

$P_g(t) = |c_g(t)|^2$, $P_e(t) = |c_e(t)|^2$ and with different $\mathrm{IRREP}_g \neq \mathrm{IRREP}_e$—this means symmetry breaking. This can be visualized by snapshots of the one-electron density $\rho(\mathbf{r}, t) = \int |\Psi(\mathbf{r}^N, \mathbf{s}^N, t)|^2 d\mathbf{s}^N d\mathbf{r}^{N-1}$ (where $\mathbf{r}^N$ and $\mathbf{s}^N$ denote the positions and spins of the electrons). In the quasi-field-free environment near t_c, the superposition state evolves with coefficients $c_g(t) = C_g e^{i\eta_g - iE_g t/\hbar}$ and $c_e(t) = C_e e^{i\eta_e - iE_e t/\hbar}$, and $\rho(\mathbf{r}, t)$ describes charge migration with period $T = h/\Delta E$ where $\Delta E = E_e - E_g$ [15,16,25–31]. The related probabilities are nearly constant, and the phase difference decreases linearly with time,

$$\Delta\eta(t) = \eta_e - \eta_g - \Delta E \cdot t/\hbar. \tag{4}$$

This allows us to choose the time delay t_d such that

$$\Delta\eta(t_c = 0) \bmod 2\pi = \{0, \pm\pi\}. \tag{5}$$

As a consequence, the coefficients $c_g(t_c)$ and $c_e(t_c)$ are real valued, except for an irrelevant global phase $\eta (= \eta_g = \eta_e \bmod \pi)$.

The second laser pulse $\epsilon_r(t)$, Eq. (1), deexcites the superposition state back to the ground state if the two conditions, Eqs. (3) and (5) are satisfied—thus it restores symmetry. In practice, condition (5) must be satisfied with precision of a few attoseconds, otherwise symmetry cannot be restored. For example, if the second pulse is fired with additional time t' at $t'_r = t_r + t'$, that means with increasing time delay $t'_d = t_d + t'$ that violates condition (5), then the final ($t'_f = t_f + t'$) population of the excited state varies periodically, with amplitude $2P_g(t_c)P_e(t_c)$ and period T,

$$P_e(t'_f) = 4P_g(t_c)P_e(t_c)\left[\frac{1}{2} - \frac{1}{2}\cos(2\pi t'/T)\right]. \tag{6}$$

The first application is to the benzene molecule. Symmetry breaking in benzene has already been documented by Ulusoy and Nest [32] in their fundamental approach to laser control of aromaticity—this motivates our choice and adaptation of their molecular model system. Initially ($t = t_i$), the molecule is in its electronic ground state S_0, with D_{6h} symmetry, see Fig. 1(a). The electric fields $\vec{\epsilon}_b(t)$ and $\vec{\epsilon}_r(t)$ of the laser pulses that break and restore this molecular symmetry are illustrated in Fig. 2(a). The laser parameters with resonant frequency defined by $\hbar\omega_c = E_e - E_g = hc/\lambda$ are listed in the Fig. 2 legend.

The pulse defined in Eq. (2) excites the benzene molecule from its initial ($t = t_i$) electronic ground state $\Psi_g = S_0$ (IRREP A_{1g}, D_{6h} symmetry) to the excited superposition state $\Psi(t_c = 0) = c_g(0)\Psi_g + c_e(0)\Psi_e$ (C_s symmetry). Relatively weak pulses with peak intensity $I = 2.6\ \mathrm{GW/cm^2}$ are applied, on a timescale where nuclear motion can safely be neglected [33,34], $t_f - t_i < 10$ fs. This yields the maximal excitation probability $P_e(t_c = 0) = 0.0037$. Here, the excited state Ψ_e is a complex-valued superposition of two real-valued degenerate excited states, $\Psi_e = \sqrt{1/2}(S_x + iS_y)$ (IRREP E_{1u}) with energy $E_e = E_x = E_y$ [16,32]. The corresponding energy gap is $\Delta E = 8.21$ eV, and the period of charge migration is $T = 504$ as. Subsequently, the pulse with electric field $\vec{\epsilon}_r(t)$ restores symmetry (D_{6h}). The population dynamics $P_e(t)$ is illustrated in Fig. 2(b).

Figure 1(a) shows snapshots of the initial and final electronic densities of benzene, together with the

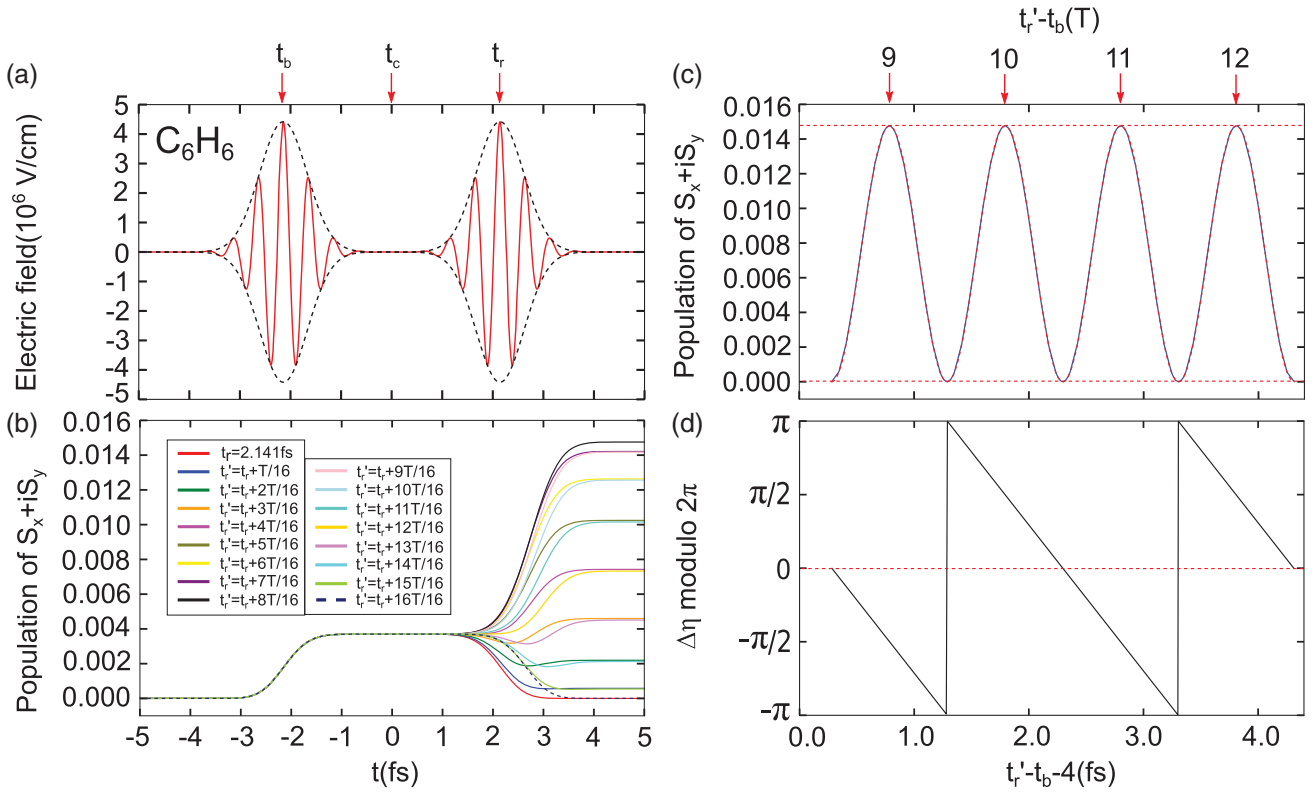

FIG. 2. Laser-driven symmetry breaking and restoration in benzene upon application of right circularly polarized pulses with amplitude $\epsilon = 4.42 \times 10^6$ V/cm, wavelength $\lambda = 151.016$ nm, and with pulse duration $\tau = 0.47$ fs. (a) Envelope and x component of the laser pulses used to break and restore symmetry at time delay $t_r - t_b$. (b) Evolution of the excited state population for various time delays, $t_r' - t_b = t_r - t_b + kT/16$, with $t_r - t_b = 4.282$ fs and period $T = 504$ as and $k \in \{0, \ldots, 16\}$. (c) Final populations [compare panel (b)] versus time delay between the pulses for symmetry breaking and restoration. (d) Phase difference (modulo 2π) at t_c', see Eq. (4).

time-dependent part of the density between the two laser pulses, which documents circular charge migration. The circulating electronic structure of the superposition state has broken symmetry (C_s) compared to the initial symmetry (D_{6h}) of benzene in its ground state S_0. Figure 2(b) also shows the population dynamics $P_e(t)$ for various cases with longer time delays $t_r - t_b + t'$. The final populations $P_e(t_f')$ [Fig. 2(c)] are in perfect agreement with the analytical result (6). The corresponding phase difference, $\Delta\eta(t_c)$ mod 2π, is documented in Fig. 2(d). These results confirm that symmetry restoration [$P_e(t_f) = 0$] is only possible for special time delays $\{t_r - t_b + kT | k \in \mathbb{N}\}$ that satisfy condition (5).

Our second proof of principle comes with both quantum dynamics simulations and a key experiment: coherent control of symmetry breaking and restoration of the ^{87}Rb atom, from isotropic electronic structure in its initial ($E_g = 0$) state $\Psi_g = 5^2S_{1/2,F=2,m_F=2}$ to anisotropic structure in the superposition state $\Psi(t) = C_g\Psi_g + C_e e^{-iE_e t/\hbar}\Psi_e$, and back to the isotropic structure. Here, $\Psi_e = 42^2D_{5/2,F=4,m_F=4}$ denotes the excited Rydberg state with energy E_e. The corresponding energy gap is $\Delta E = 4.1688969$ eV [35], the period is $T = 0.9920292$ fs. Excitations of Rydberg states of ^{87}Rb have already discovered various fundamental effects [36–40]—this motivates our choice of this atomic model system. Excitation of Ψ_e is by a laser pulse, which consists of two right circularly polarized subpulses labeled 1 and 2, as illustrated in Fig. 3(a). For comparison, counterrotating right and left circularly polarized laser pulses open complementary opportunities, e.g., switching intramolecular ring currents and induced magnetic fields [41], the production of electron vortices [42], selective generation of circularly polarized high harmonics depending on the conformity of the symmetries of the laser field and the molecule [43–45], and time-dependent monitoring of symmetry breaking [46]. For the present application, symmetry breaking after the first laser pulse is monitored by measuring the nonzero population of the excited state, as documented in Fig. S1 of the Supplemental Material [24]. The resulting evolution of the electron wave packet is illustrated in Fig. 1(b).

Laser parameters for the calculation are given in the caption of Fig. 3 (see the Supplemental Material [24] with Refs. [47–51] for the derivation of these parameters

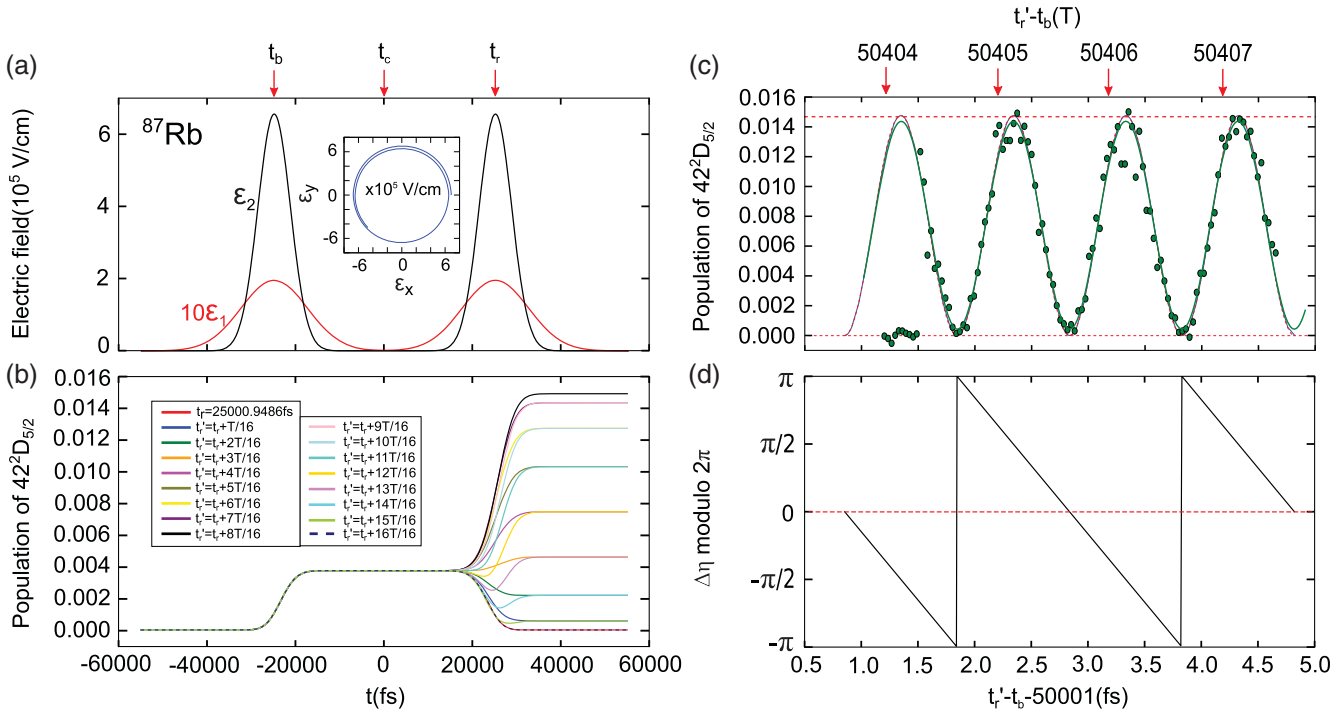

FIG. 3. Laser-driven symmetry breaking and restoration in ^{87}Rb. Each pulse is composed of two right circularly polarized subpulses with amplitudes $\epsilon_1 = 1.98 \times 10^4$ and $\epsilon_2 = 6.648 \times 10^5$ V/cm, wavelength $\lambda_1 = 779.17$ and $\lambda_2 = 480.995$ nm, pulse durations [Eq. (2)] $\tau_1 = 7.4953$ and $\tau_2 = 3.677$ ps. (a) Envelopes of the two subpulses used to break and restore symmetry, with time delay $t_r - t_b$. The inset shows the components ϵ_x and ϵ_y of the net electric field of the two corotating right circularly polarized subpulses during one period τ_1, starting at $t = t_b$. (b) Population evolution of the excited Rydberg state $\Psi_e = 42^2D_{5/2,F=4,m_F=4}$ for various time delays, $t_r' - t_b = t_r - t_b + kT/16$, with $t_r - t_b = 50.00189714$ ps and $T = 0.99202924$ fs and $k \in \{0, \ldots, 16\}$. (c) Experimental population dynamics obtained by time-domain Ramsey interferometry with attosecond time resolution around the time delay $t_r' - t_b \sim 50$ ps. The green curve fitted to the experimental data (green dots) reveals a high contrast (~0.94) of the Ramsey interferogram, which is compared with the numerical and analytical calculations (red and blue curves, respectively). The vertical scale of the experimental data and fitted curve was arbitrary and adjusted so that their mean value became equal to those of the numerical and analytical curves. The horizontal position of the experimental data as well as their fitted curve was then moved so that the phase of the fitted curve matched those of the numerical and analytical curves. The first 10 points were measured with the excitation laser pulses blocked, showing the zero level of the measured signal. See the Supplemental Material [24] for the details. (d) Phase difference (modulo 2π), see Eq. (4).

and for the numerics). Circular charge migration of the superposition state with broken symmetry is illustrated in Fig. 1(b). Figure 3(b) shows the population dynamics $P_e(t)$ for various cases with longer time delays $t_r - t_b + t'$. The final population $P_e(t_f')$ is shown in Fig. 3(c) as a function of the time delay. The corresponding phase difference, $\Delta\eta(t_c)$ mod 2π, is documented in Fig. 3(d). Similar to benzene, the final population of the excited Rydberg state is zero at specific time delays at which symmetry restoration is realized.

We demonstrate the feasibility of symmetry restoration by measuring the time-delay dependence of the population $P_e(t_f')$ in the excited Rydberg state of the ^{87}Rb atom by time-domain Ramsey interferometry with attosecond precision [39]. The experimental methods were similar to those of Ref. [39]; see Supplemental Material [24] for details. Briefly, a cold ensemble of $\sim 4 \times 10^5$ ^{87}Rb atoms was prepared in an optical dipole trap with its temperature estimated to be ~100 μK, and then released and expanded before irradiating the symmetry-breaking laser pulse. The atoms were optically pumped to the hyperfine state of the ground state $\Psi_g = 5^2S_{1/2,F=2,m_F=2}$ and excited mostly to the Rydberg state $\Psi_e = 42^2D_{5/2,F=4,m_F=4}$ via a two-photon transition using right circularly polarized picosecond laser pulses with their center wavelengths tuned to ~779 and ~481 nm, respectively. The time-domain Ramsey interferogram was measured with a pair of the two-photon excitations with time delay $t_r' - t_b$ stabilized on the attosecond timescale with our highly stabilized interferometer [39]. The estimation of this attosecond stability is described in the Supplemental Material [24]. By scanning the time delay $t_r' - t_b$ in steps of ~30 as, we measured the Rydberg population $P_e(t_f')$ that survived after the pair of excitations by field ionization [39]. Figure 3(c) shows the Ramsey interferogram measured as a function of time delay at $t_r' - t_b \sim 50$ ps. We obtained the contrast of the measured oscillation by sinusoidal fitting to be 0.94 ± 0.02, where the contrast was defined to be the ratio of the amplitude of

the fitted sinusoidal function to its mean value. The high contrast is a *conditio sine qua non* for the preparation of the final electronic state with the target symmetry, almost without any contamination by states with different IRREPs. If the delay times do not satisfy condition (5), then symmetry breaking is measured, by means of the spectroscopic selection rules. Specifically, the maximum value of the final population of the excited state $P_e(t'_f)$ is nonzero in Fig. 3(c). Its population after the first laser pulse $P_e(t_c) \propto |\langle \Psi_g | H_{\rm int} | \Psi_e \rangle|^2$, cf. Eq. (6), and the corresponding transition matrix element are, therefore, also nonzero, $\langle \Psi_g | H_{\rm int} | \Psi_e \rangle \neq 0$. Here, $H_{\rm int}$ denotes the atom-laser interaction with two right circularly polarized photons. Since Ψ_g has the highest symmetry, [IRREP $D^{(0)}$ in $S_0(3)$], the product integral theorem together with angular momentum conservation then tell us that the IRREP of Ψ_e is $D^{(2)}$, different from the symmetry $D^{(0)}$ of the ground state. Gratifyingly, this is indeed the symmetry of the excited state, $42^2D_{5/2,F=4,m_F=4}$. The superposition state $c_g\Psi_g + c_e\Psi_e$ cannot have the isotropic IRREP $D^{(0)}$ of the ground state—symmetry was broken by the first laser pulse. Our results therefore infer the experimental feasibility of the symmetry breaking and restoration.

In summary, this Letter demonstrates electronic structure symmetry restoration using a two-pulse coherent control strategy by numerical simulations for benzene and ^{87}Rb. The latter theoretical findings are confirmed experimentally by high-contrast time-dependent Ramsey interferometry with precision in the attosecond. Symmetry breaking and symmetry restoration in symmetric molecules provide sufficient (though not exclusive [15,31]) tools to initiate and to stop charge migration.

The present simple examples allow various extensions to symmetry breaking and restoration with more demanding applications, e.g., with multiple pulses for symmetry breaking that involve several excited states and corresponding incommensurable frequencies. Thus, Ulusoy and Nest [32] have designed a series of three laser pulses for control of aromaticity of benzene—the final state corresponds to $D_{6h} \rightarrow C_{2v}$ symmetry breaking (different from the present case $D_{6h} \rightarrow C_s$). Here one could restore symmetry ($C_{2v} \rightarrow D_{6h}$) by application of another three pulses in reverse order, with proper observation of the conditions of temporal symmetry Eq. (3), and phase matching Eq. (5), and possibly alternative control knobs, e.g., the carrier envelope phases. The series of pulses for symmetry breaking may be replaced by a single pulse designed by means of optimal control [32], and as a working hypothesis, the three pulses for symmetry restoration may also be replaced by a single optimal laser pulse [9], and this could reveal new mechanisms for symmetry restoration [52,53].

We are grateful to Professor M. Weidemüller (Heidelberg) and Dr. T. Grohmann (Berlin) for stimulating discussions, and to Professor D. Haase (Berlin), Professor I. Hertel (Berlin) and PD. Dr. M. Leibscher (Kassel) for helpful guidance to part of the literature. Generous financial support by the National Key Research and Development Program of China (Grant No. 2017YFA0304203), the Program for Changjiang Scholars and Innovative Research Team (IRT-17R70), the National Natural Science Foundation of China (Grant No. 11434007), the National Science Foundation of China (Grant No. 61505100), the 111 Project (Grant No. D18001), the China Scholarship Council, the Shanxi 1331 Project Key Subjects, the Deutsche Forschungsgemeinschaft (Project No. Tr 1109/2-1), Alexander von Humboldt Foundation ("Humboldt Research Award"), CREST-JST, JSPS Grants-in-Aid for "Specially Promoted Research" Grant No. 16H06289 and for "Young Scientist (B)" Grant No. 17K14365, and Photon Frontier Network by MEXT is also gratefully acknowledged.

*Corresponding author.
jmanz@chemie.fu-berlin.de
†Corresponding author.
ohmori@ims.ac.jp

[1] M. Ivanov, P. B. Corkum, and P. Dietrich, Laser Phys. **3**, 375 (1993).
[2] T. C. Weinacht, J. Ahn, and P. H. Bucksbaum, Phys. Rev. Lett. **80**, 5508 (1998).
[3] N. Elghobashi, L. González, and J. Manz, J. Chem. Phys. **120**, 8002 (2004).
[4] Y. Arasaki and K. Takatsuka, Phys. Chem. Chem. Phys. **12**, 1239 (2010).
[5] Y. Arasaki, K. Wang, V. McKoy, and K. Takatsuka, Phys. Chem. Chem. Phys. **13**, 8681 (2011).
[6] A. S. Alnasser, M. Kübel, R. Siemering, B. Bergues, N. G. Kling, K. J. Betsch, Y. Deng, J. Schmidt, Z. A. Alahmed, A. M. Azzeer, J. Ullrich, I. Ben-Itzhak, R. Moshammer, U. Kleineberg, F. Krausz, R. de Vivie-Riedle, and M. F. Kling, Nat. Commun. **5**, 3800 (2014).
[7] Y. Pertot, C. Schmidt, M. Matthews, A. Chauvet, M. Huppert, V. Svoboda, A. Conta, A. Tehlar, D. Baykusheva, J.-P. Wolf, and H. J. Wörner, Science **355**, 264 (2017).
[8] edited by W. P. Schleich and H. Walther, *Elements of Quantum Information* (Wiley-VCH, Weinheim, 2007).
[9] C. Brif, R. Chakrabarti, and H. Rabitz, New J. Phys. **12**, 075008 (2010).
[10] M. Shapiro and P. Brumer, *Quantum Control of Molecular Processes*, 2nd ed. (WILEY-VCH, Weinheim, 2012).
[11] R. Woodward and R. Hoffmann, *Die Erhaltung der Orbitalsymmetrie* (Verlag Chemie, Weinheim, 1970).
[12] E. E. Campbell, H. Schmidt, and I. Hertel, Adv. Chem. Phys. **72**, 37 (1998).
[13] E. Halevi, *Orbital Symmetry and Reaction Mechanism: The OCAMS View* (Springer Verlag, Berlin, 1992).
[14] S. Al-Jabour and M. Leibscher, J. Phys. Chem. A **119**, 271 (2015).
[15] S. Chelkowski, G. L. Yudin, and A. D. Bandrauk, J. Phys. B **39**, S409 (2006).

[16] D. Jia, J. Manz, B. Paulus, V. Pohl, J. C. Tremblay, and Y. Yang, Chem. Phys. **482**, 146 (2017).
[17] G. Alber, H. Ritsch, and P. Zoller, Phys. Rev. A **34**, 1058 (1986).
[18] L. D. Noordam, D. I. Duncam, and T. F. Gallagher, Phys. Rev. A **45**, 4734 (1992).
[19] P. B. Corkum, Phys. Rev. Lett. **71**, 1994 (1993).
[20] P. B. Corkum and F. Krausz, Nat. Phys. **3**, 381 (2007).
[21] F. Krausz and M. Ivanov, Rev. Mod. Phys. **81**, 163 (2009).
[22] S. Chelkowski, T. Bredtmann, and A. D. Bandrauk, Phys. Rev. A **85**, 033404 (2012).
[23] T. Schultz and M. Vrakking, *Attosecond and XUV Physics* (WILEY-VCH, Weinheim, 2014).
[24] See Supplemental Material at http://link.aps.org/supplemental/10.1103/PhysRevLett.121.173201 for Experimental methods; Derivation of conditions for symmetry restoration; Models and methods.
[25] L. S. Cederbaum and J. Zobeley, Chem. Phys. Lett. **307**, 205 (1999).
[26] I. Barth and J. Manz, Angew. Chem. Int. Ed. **45**, 2962 (2006).
[27] F. Remacle and R. D. Levine, Proc. Natl. Acad. Sci. U.S.A. **103**, 6793 (2006).
[28] M. Kanno, H. Kono, and Y. Fujimura, Angew. Chem. Int. Ed. **45**, 7995 (2006).
[29] P. M. Kraus, B. Mignolet, D. Baykusheva, A. Rupenyan, L. Horny, E. F. Penka, G. Grassi, O. I. Tolstikhin, J. Schneider, F. Jensen, L. B. Madsen, A. D. Bandrauk, F. Remacle, and H. J. Wörner, Science **350**, 790 (2015).
[30] K. Ueda, Science **350**, 740 (2015).
[31] N. V. Golubev, V. Despré, and A. Kuleff, J. Mod. Opt. **64**, 1031 (2017).
[32] I. S. Ulusoy and M. Nest, J. Am. Chem. Soc. **133**, 20230 (2011).
[33] H. Mineo, S. H. Lin, and Y. Fujimura, Chem. Phys. **442**, 103 (2014).
[34] V. Despré, A. Marciniak, V. Loriot, M. C. E. Galbraith, A. Rouzée, M. J. J. Vrakking, F. Lépine, and A. I. Kuleff, J. Phys. Chem. Lett. **6**, 426 (2015).
[35] W. Li, I. Mourachko, M. W. Noel, and T. F. Gallagher, Phys. Rev. A **67**, 052502 (2003).
[36] A. Marian, M. C. Stowe, J. R. Lawall, D. Felinto, and J. Ye, Science **306**, 2063 (2004).
[37] D. Tong, S. M. Farooqi, J. Stanojevic, S. Krishnan, Y. P. Zhang, R. Côté, E. E. Eyler, and P. L. Gould, Phys. Rev. Lett. **93**, 063001 (2004).
[38] K. Singer, M. Reetz-Lamour, T. Amthor, L. Marcassa, and M. Weidemüller, Phys. Rev. Lett. **93**, 163001 (2004).
[39] N. Takei, C. Sommer, C. Genes, G. Pupillo, H. Goto, K. Koyasu, H. Chiba, M. Weidemüller, and K. Ohmori, Nat. Commun. **7**, 13449 (2016).
[40] J. Wolters, G. Buser, A. Horsley, L. Béguin, A. Jöckel, J.-P. Jahn, R. J. Warburton, and P. Treutlein, Phys. Rev. Lett. **119**, 060502 (2017).
[41] I. Barth and J. Manz, *Progress in Ultrafast Intense Laser Science VI* (Springer, Berlin, 2010), Chap. 2.
[42] J. M. N. Djiokap, S. X. Hu, L. B. Madsen, N. L. Manakov, A. V. Meremianin, and A. F. Starace, Phys. Rev. Lett. **115**, 113004 (2015).
[43] F. Mauger, A. D. Bandrauk, and T. Uzer, J. Phys. B **49**, 10LT01 (2016).
[44] X. Liu, X. Zhu, L. Li, Y. Li, Q. Zhang, P. Lan, and P. Lu, Phys. Rev. A **94**, 033410 (2016).
[45] K.-J. Yuan and A. D. Bandrauk, Phys. Rev. A **97**, 023408 (2018).
[46] D. Baykusheva, M. S. Ahsan, N. Lin, and H. J. Wörner, Phys. Rev. Lett. **116**, 123001 (2016).
[47] M. L. Zimmerman, M. G. Littman, M. M. Kash, and D. Kleppner, Phys. Rev. A **20**, 2251 (1979).
[48] M. Marinescu, H. R. Sadeghpour, and A. Dalgarno, Phys. Rev. A **49**, 982 (1994).
[49] T. F. Gallagher, *Rydberg Atoms* (Cambridge University Press, Cambridge, England, 2005).
[50] D. A. Steck, http://steck.us/alkalidata/.
[51] E. Anderson, Z. Bai, C. Bischof, S. Blackford, J. Demmel, J. Dongarra, J. D. Croz, A. Greenbaum, S. Hammarling, A. McKenney, and D. Sorensen, *LAPACK Users'Guide* 3rd ed. (Society for Industrial and Applied Mathematics, Philadelphia, PA, 1999).
[52] N. Došlić, O. Kühn, J. Manz, and K. Sundermann, J. Phys. Chem. A **102**, 9645 (1998).
[53] C. Daniel, J. Full, L. González, C. Lupulescu, J. Manz, A. Merli, Š. Vajda, and L. Wöste, Science **299**, 536 (2003).